



SHROUDED KINETIC TURBINES OPTIMIZATION FOR RUN THE RIVER AND TIDAL PICO-HYDROPOWER

Robert Vincent Clarke

School of Engineering and Architecture, Alma Mater Studiorum University of Bologna, Forlì Campus, Via Fontanelle, Italy

E-Mail: robertvclarke@gmail.com

ABSTRACT

At our current state of technological development, the designs being proposed for the “channeling of a turbine” based on wind power, commonly called DAWT (Diffuser-Augmented) or CWAT (Compact-Acceleration), utilize a diffuser (divergent) shaped as an airfoil. Further developments of the concept have brought about the introduction of other winged-profiled ring structures behind or in front of the entrance to the divergent making the design more complicated as well as more expensive due to the difficulty of producing correct contours. Even though this results in an increase in power, it usually is limited to slightly more than a four-fold increase at most. In addition, brims (wing-lens) have been recently added around the external edges of the diffuser. Nonetheless, brims thus designed, are not suitable for use in a river due to the significant stress that the structure as a whole needs to withstand. No design, proposed until now, includes a convergent at the entrance to a turbine due to the obstruction effect that it has on the flow of water into the turbine, slowing it down and thereby reducing the acceleration produced by the “channelizing” divergent. This article will introduce an innovative convergent-divergent to which can be inserted a hydro-kinetic turbine which will increase the maximum output power available 12.7 times compared with a free turbine.

Keywords: diffuser-augmented, compact-acceleration, hydro-power, run the river, low head, water powered turbine.

INTRODUCTION

Hydro-electric power was the first source of renewable energy to be used on a large scale and at the moment represents about 20% of world energy production. Hydro-electric power represents the principal alternative source of energy to fossil fuels used in Italy and produces 15% of the national needs. According to GSE sources [5], 18,232 MW are produced from 303 stations larger than 10 MW, 781 between 1 and 10 MW, and 1886 stations under 1 MW. In Figure-1 is shown the distribution, by region, of class power percentage, installed in Italy in 2012.

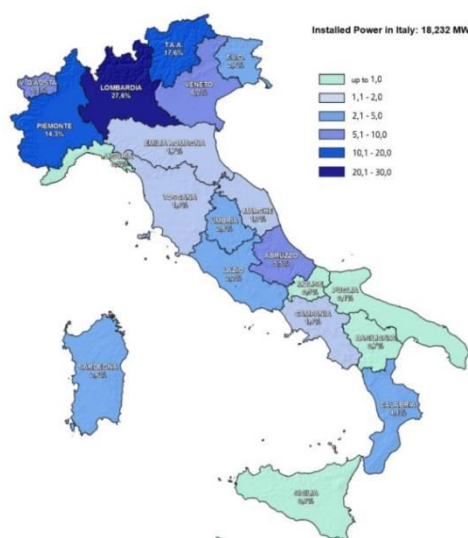


Figure-1. Distribution by region of hydro-electric power in Italy (2012) [5].

In any event, hydro-electric power, compared with other forms of renewable energy, has reached its

maximum level of exploitation of the resources available. Most large-scale power stations have already been completed. The only road left is to develop so-called “small hydro stations”. In fact, an enormous potential for hydro-electric energy exists in the numerous rivers, waterways and artificial irrigation canals in Italy (an around the World) where it is not practical to build a dam. In this situation, a conventional turbine, whether it be a Pelton, a Francis or a Kaplan type, would need a piezometric head of at least few meters to make it function and thus would be inefficient in these types of waterways. It is for this reason, together with an ever increasing desire to safe-guard the environment that a lot of attention in the last few decades has been drawn to free flow turbines. These turbines convert the kinetic energy of a moving mass of fluid directly into mechanical energy made available to a shaft, without interrupting the natural flow, much like a wind turbine. This direct conversion has a number of advantages, above all, the elimination of the need for large public works projects to block the flow of water which has significant environmental impact and high investment costs. In addition, free flow turbines allow for a greater range of choice of potential sites. These turbines, also called hydro-kinetic turbines, work due to concepts derived from aerogenerators and until now have been based on designs of wind rotors. As of today, numerous and varied designs have been proposed. These designs range from the very simple concept of waterwheels which work by force of resistance to rotors (placed either horizontally or vertically with respect to a fluid flow) that use a with an airfoil-shape blade to exploit the lift force so that it rotates with a speed greater than the flow which strikes them. These turbines have a verified power coefficient (C_p) ranging from 0.2 for resistance-based turbines to a maximum of 0.4 for lift-based turbines. Shrouded turbines are not subject to the so-called



Lanchester-Benz limit which establishes a maximum of 59.3% as the amount of kinetic energy that can be converted into mechanical energy from any flow source according to the single disk actuator theory of Rankine-Froude [6]. For encased turbines the theoretical limit depends on the difference in pressure created between the inlet and the outlet of the device used and the mass of the flow going through it or in other words, the form or shape of the conduit and the ratio of the entrance area and the area swept by the turbine blades. Studies by Riegler (1983) [8] show that “channelizing” a turbine (in his case one with a horizontal axis) improves the power coefficient of a factor of 1.96; 3.3 times the Betz limit. This seems possible due to the fact that the flow is “sucked” from a wider up stream area compared with the flow intercepted from the frontal area of a rotor in a free flow. After all, this doesn’t mean that the Betz limit has been violated. In fact, the streamtube has been modified as shown in Figure-2.

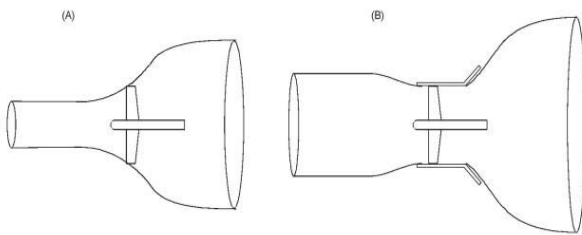


Figure-2. Streamtube inside a turbine (a) free and (b) shrouded^[3].

The kinetic energy of any objects whatsoever of a given mass (m) in movement at an average velocity (V) is defined by the following expression:

$$E_K = \frac{1}{2}mV^2 \quad (1)$$

Hence the theoretical power that can be extracted from a flow of water is as follows:

$$P_{Th} = \frac{dE_k}{dt} = \frac{1}{2}\dot{m}V^2 \quad (2)$$

Considering that the flow rate of a mass of fluid with a density of (ρ), across a section (A), with a velocity (V) could be expressed as follows:

$$\dot{m} = \rho AV \quad (3)$$

Combining the two preceding equations we obtain a more explicit expression of power:

$$P_{Th} = \frac{1}{2}\rho AV^3 \quad (4)$$

Equation (4) illustrates the power available in any fluid. Therefore, it describes the power of water that flows by a rotor with frontal section A for any given velocity V . It can easily be seen that in order to obtain greater power, given the same density, higher velocity and longer blades are needed to obtain an increase in frontal area. In

particular, even a minimum variation in fluid speed leads to a noticeable increase of power available as this is proportional to the cube of itself. In any event, (4) represents the energy that can be extracted assuming that the conversion process is 100% efficient. A parameter for evaluating the efficiency of a turbine that exploits kinetic energy is the power coefficient (C_p) defined as the ratio between the useful power supplied by the machine and the power made available by the flow:

$$C_p = \frac{P_{turbine}}{P_{Th}} \quad (5)$$

Seeing as how the power of the rotor is represented by the torque (T) multiplied by the angular velocity (ω) around which it rotates, the coefficient can be expressed more explicitly as:

$$C_p = \frac{T\omega}{\frac{1}{2}\rho AV^3} \quad (6)$$

From the theoretical equation (4) which expresses the useful power that is possible to extract from a mass of water in movement it is clear that there are two parameters upon which we can work: 1) the frontal area of the rotor which intercepts the flow and 2) the average velocity of the fluid. Therefore, considering the use of such turbines in rivers two problems arise essentially. First, the speed of the current of the rivers is very low; therefore, the Hydro-kinetic turbines can not convert enough energy. Second, they have low depths according the rotor size (and therefore the frontal area) must remain compulsorily reduced. Thus it only remains to focus on the flow speed parameter.

Basic idea and the Venturi effect concept

This suggests that a device which is able to accelerate, direct and channel the flow in turbomachinery can extract more energy and make more power available to the shaft. The aim of this study is to devise a pico-hydroelectric power system (nominal power < 5kW) which is both simple and economic and capable of increasing the power of any turbine whatsoever, whether it has a horizontal (HAWT) or a vertical (VAWT) shaft. Such a system could be used mainly in large rivers where there is no useful fall or drop in water level, keeping the rotor size to the minimum possible while having no impact whatsoever on the environment. The decision was to shape the device to fit a three-blade, free flow turbine with a vertical shaft (H-Darrieus) derived from a wind turbine with a symmetric NACA 0021 blade. The initial choice fell on a straight bladed Darrieus type turbine because of its simple design and for the advantage that it keeps the generator and the different electrical parts above water level, saving on water-proofing and easing access for eventual maintenance. In addition, it is possible to add more turbines while using only a single shaft and generator, increasing the nominal power output of the entire system. The basic idea is to enclose the rotor in a convergent-divergent subsonic tube of suitable geometric



design in order to exploit the Venturi effect. In contrast to wind power, where the large diameters of the rotors preclude the use of encased devices, in the field of hydro-electrics, especially in rivers, the diameter of the rotors is limited, instead, by the transversal section of the riverbed and it is, therefore, advantageous to shroud the turbines to increase the velocity of the current and as a consequence augment the power extracted. What is more, the density of water is about 800 times that of air and, therefore, such machines can, all conditions being equal, have greatly reduced dimensions and are more efficient at low speeds than wind turbines. For example, a current of water of only 1 m/s has a power of about 500 W/m as compared to little more than 0.6 W/m for wind.

The Venturi effect (G.B. Venturi, 1746-1822) is a phenomenon that takes place when an incompressible fluid passes through a tube or conduit with a constriction in one section. The speed of the flow in passing through the narrowing must increase since it must satisfy the equation of continuity while the pressure will be reduced in order to respect the conservation of energy. The gain in kinetic energy is balanced by the drop in (static) pressure.

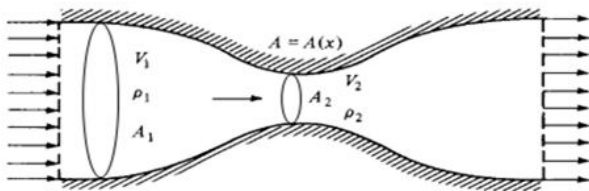


Figure-3. Drawing of a flow in a conduit with a constriction.

A Venturi tube is a conduit in which a convergent section is followed by a divergent section as shown in Figure-2. Given the geometric characteristics we can assume that the variables of the motion field are a function of only the direction (X). This type of flow is called quasi-one dimensional which in our case ends up being a good approximation of a tri-dimensional flow. Taking into consideration the continuity equation, with the hypothesis of steady flow, in the following form:

$$\rho_i A_i V_i = \text{const} \quad (7)$$

Where the density (ρ) is constant for the hypothesis of an incompressible flow, (A) is the cross-section area and (V) the average velocity of the flow. From Bernoulli's equation we have that:

$$p_i + \frac{1}{2} \rho_i V_i^2 + \rho_i g h_i = \text{const} \quad (8)$$

Where the first term is the static pressure, the second term is the dynamic pressure and the third term is the hydrodynamic pressure. Taking into consideration a horizontal tube ($h=0$) and keeping true to the assumption of an incompressible flow, results in the variation of the (static) pressure between the two sections A_1 , A_2 being:

$$\Delta p = p_2 - p_1 = \frac{1}{2} \rho_1 V_1^2 - \frac{1}{2} \rho_2 V_2^2 \quad (9)$$

From the equation of continuity (7) it is easy to obtain the relation between the velocity V_1 at the opening and the velocity V_2 in the constriction as shown in the following:

$$V_1 = V_2 \frac{A_2}{A_1} \quad (10)$$

Which when substituted for V_1 in (9) results in a clear dependency of the dimensions of the sections:

$$\Delta p = p_2 - p_1 = \frac{1}{2} \rho V_2^2 \left[\left(\frac{A_2}{A_1} \right)^2 - 1 \right] \quad (11)$$

as a consequence we have that:

$$\frac{A_2}{A_1} > 1 \text{ Expansion } p \uparrow, V \downarrow \quad (12)$$

$$\frac{A_2}{A_1} < 1 \text{ Reduction } p \downarrow, V \uparrow \quad (13)$$

The two relationships (12) and (13), define the subsonic behavior of the fluid inside the Venturi tube for which in a convergent conduit the velocity increases while the static pressure diminishes to a minimum value in correspondence of the throat; conversely, in a divergent conduit, the static pressure increases in connection with a reduction of velocity (and therefore of dynamic pressure). Defining the contraction ratio (CR) as the ratio between the area of the entrance section A_1 and the throat section A_2 :

$$CR = \frac{A_1}{A_2} \quad (14)$$

We have that theoretically an increase in contraction leads to a greater increase in velocity and as a consequence we obtain a greater increase in power as shown in the following:

$$\frac{P_{2Th}}{P_{1Th}} = \frac{A_2 V_2^3}{A_1 V_1^3} = CR^2 \quad (15)$$

In order to have a starting point on size and geometry of the conduit, the European standard ISO 5167-3:2003 [4] (Figure-4) was referred to. This standard defines terms, symbols and general principles for the methods of measurement and calculation of the flow rate of a fluid which runs through a conduit by means of differential pressure devices (openings, nozzles and Venturi tubes) when they are inserted into a circular cross-section. Furthermore, the standard specifies the general limits of the dimensions of the tube and the number of Reynolds for which these devices can be used. In particular, part three of this text establishes the limitations and the geometry of the Venturi nozzle as described in Table-1, optimized in loss due to friction and separation, based on numerous experiments. The choice fell on a



Venturi nozzle due not only to its convergent-divergent shape but also to the fact that it has an internal throat section long enough to house a Darrieus type turbine.

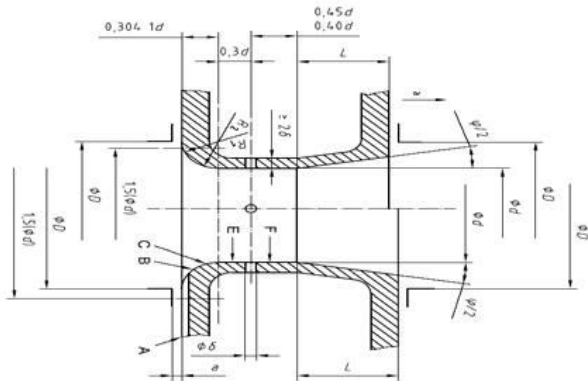


Figure-4. Venturi nozzle geometry according to ISO 5167-3 [4].

Table-1. Limitations ISO 5167-3 [4].

$0.065 \leq D \leq 0.500 \text{ m}$	Inlet section diameter
$d \geq 0.050 \text{ m}$	Throat section diameter
$0.316 \leq \beta \leq 0.775$	$\beta = \text{ratio } d/D$
$\phi_1 \leq 30^\circ$	Angle diffuser opening
$1.5 \cdot 10^5 \leq Re_D \leq 2 \cdot 10^6$	Reynolds number referred to D
$M \leq 0.3$	Mach number
$Ra \leq 6.125 \cdot 10^{-2}$	Surface roughness

To ensure that in our model the flow behavior meets the standard conditions, we have considered the concept of flows similarity. An iterative program in *Matlabcode* [2] was written to select the diameters and the optimum contraction ratio CR, respecting the ISO 5167-3. A further program instead returns the optimal size of the convergent-divergent according to the diameter of the used turbine. This has served to draw in *SolidWorks* the device and test its effectiveness by *CFD Simulation Flow* program.

Flow accelerator: Evolution of the Venturi nozzle

This study began by creating diverse models of convergents-divergents in *SolidWorks* having the same throat section diameter ($d=0.9 \text{ m}$) and angle of divergence ($\phi_1=30^\circ$) nevertheless with different contraction ratio to determine the most efficient, whether with a circular or a square-shaped throat, with the thought of using them for any type of turbine whether it be VAWT or HAWT. It was found that the best form for both the opening and the divergent was circular as it was far superior to a square shape (Figure-5). The tests were carried out with a flow velocity of 1.2 m/s, which is the average velocity calculated for the Po River (North Italy). The results shown in Table-2 and plotted on Figures 7 and 8 indicate that the most efficient contraction is found to be at

$CR=2.35$. Furthermore, it was determined that the best angle of divergence was $\phi_1=20^\circ$ (see Figure-9).

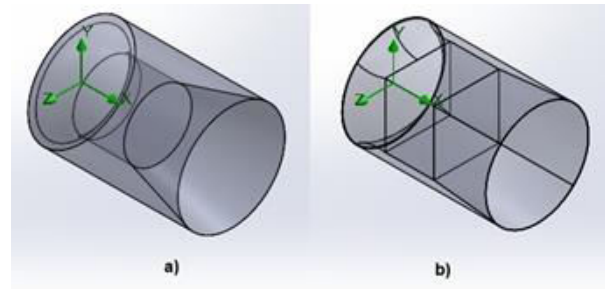


Figure-5. First model in 3D of a throat section a) circular b) square (isometric view) [2].

The simulation goal was to determine the velocity at the beginning of the throat section since this would first hit the blade of the turbine, and the velocity in the immediate area of the opening. To determine these velocities, the values obtained in six discrete points along the opening (YZ plane of the throat and entrance) were calculated using the following arithmetic average:

$$V_{(m,i)} = \frac{v_i + v_{(i+1)}}{2} \tag{16}$$

After which a weighted average was calculated with respect to the areas (see Figure-6) as follows:

$$V_m = \frac{\sum(V_{(m,i)} \cdot dA_i)}{A} \tag{17}$$

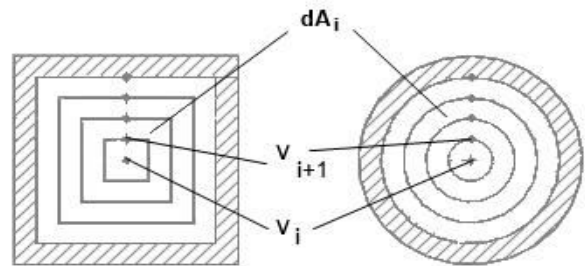


Figure-6. Average weighted velocity with respect to area [2].

Some parameters of comparison [1] derived from the average calculated velocities described in the manner above were then taken into consideration in order to evaluate the different configurations. An initial term to express the increase in velocity is defined by the ratio between the calculated velocity in the throat and the asymptotic speed of the flow;

$$C_A = \frac{v_m}{v_\infty} \tag{18}$$

a second term is defined as the theoretical flow velocity in the throat section, if at the entrance it had the asymptotic speed of the flow, divided by the real calculated velocity in the throat section; it expresses the blocking effect, in



other words, the tendency of the flow to pass around the structure rather than through, due to the increase of contraction;

$$B = \frac{V_{2Th}}{V_m} \tag{19}$$

While with the ratio between the averages calculated velocity at the entrance and the asymptotic speed of the flow we express the “suction” effect that is seen in the throat due to the particular geometry of the structure in contrast to the blocking effect *B*:

$$S_A = \frac{V_{minlet}}{V_\infty} \tag{20}$$

Intuitively, we expect that with an increase in contraction there would be a corresponding increase in velocity. However, the resistance increases with the result that the mass of fluid tends to flow around the structure rather than through it. Taking these two aspects into consideration we can state that maximum efficiency is

obtained by maximizing the ratio *C_A/B* and how much the term *S_A* nears unity. Another aspect to consider is how much the contraction can increase the energy of the flow. Keeping in mind that the power obtainable can be written solving the mass, we have:

$$P_2 = \frac{1}{2} \rho A_2 (V_m)^3 = \frac{dE}{dt} = \frac{1}{2} \frac{dm_2}{dt} (V_m)^2 \tag{21}$$

Where, $dm_2 = \rho A_2 V_m$. we can therefore introduce a parameter that defines the amplification of the power of the flow as follows:

$$P_A = \frac{\frac{1}{2} \frac{dm_2}{dt} (V_m)^2}{\frac{1}{2} \frac{dm_{fluid}}{dt} (V_\infty)^2} \tag{22}$$

Where the denominator refers to the power obtainable from an undisturbed flow having established $dm_{fluid} = \rho A_1 V_\infty$.

Table-2. Results of the average velocities a) sect. circular throat b) sect. square throat (d=0.9 m) ^[2].

a)	V _m ⁽¹⁷⁾	V _{2(Th)}	C _A ⁽¹⁸⁾	B ⁽¹⁹⁾	C _A /B	P _A ⁽²²⁾
CR 2.0	1.7174	2.40	1.43	1.40	1.02	1.47
CR 2.5	1.7905	3.00	1.49	1.68	0.89	1.33
CR 3.0	1.8465	3.60	1.54	1.95	0.79	1.21
CR 3.7	1.9177	4.44	1.60	2.32	0.69	1.10
CR 4.0	1.8732	4.80	1.56	2.56	0.61	0.95
CR 5.0	1.9294	6.00	1.61	3.11	0.52	0.83
CR 5.5	1.7590	6.60	1.47	3.75	0.39	0.57
CR 5.5*	1.8471	6.60	1.54	3.57	0.43	0.66
CR 7.0*	1.9306	8.40	1.61	4.35	0.37	0.59

*d=0.5 m

b)	V _m ⁽¹⁷⁾	V _{2(Th)}	C _A ⁽¹⁸⁾	B ⁽¹⁹⁾	C _A /B	P _A ⁽²²⁾
CR 2.00	1.6093	2.40	1.34	1.49	0.90	1.21
CR 2.15	1.6585	2.58	1.38	1.56	0.89	1.23
CR 2.25	1.6845	2.70	1.40	1.60	0.88	1.23
CR 2.35	1.8337	2.82	1.53	1.54	0.99	1.52
CR 2.50	1.8451	3.00	1.54	1.63	0.95	1.45
CR 2.75	1.7647	3.30	1.47	1.87	0.79	1.16

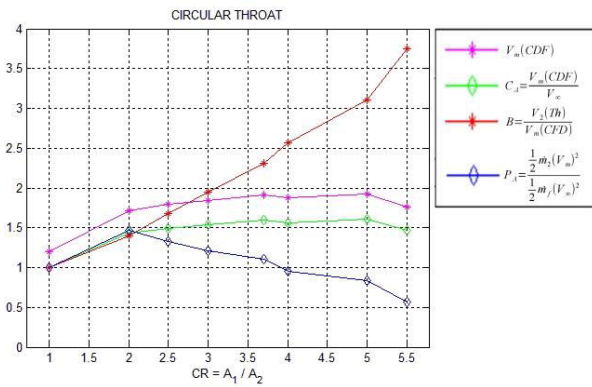


Figure-7. Trend of parameters (Circular throat).

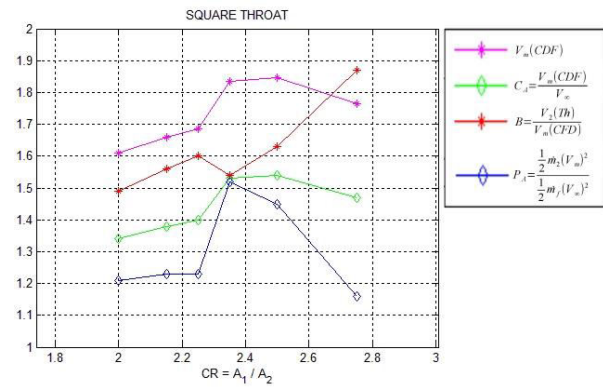


Figure-8. Trend of parameters (Square throat).

Table-3. Results of average velocities calculated from the simulations by reducing the divergence angle ϕ_1 (d=1.2 m) [2].

CR 2.35	$V_m(17)$	$V_2(Th)$	$C_A(18)$	$B(19)$	C_A/B	$P_A(22)$
$\phi_1=30^\circ$	1.7144	2.82	1.43	1.64	0.87	1.24
$\phi_1=24^\circ$	1.8294	2.82	1.52	1.54	0.99	1.51
$\phi_1=20^\circ$	1.9899	2.82	1.66	1.42	1.17	1.94
$\phi_1=18^\circ$	1.9398	2.82	1.62	1.45	1.11	1.80

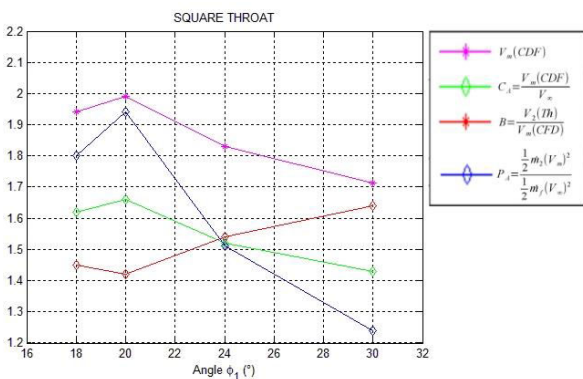


Figure-9. Trend of parameters with respect to divergent angle ϕ_1 .

Increasing the contraction, the blocking effect prevails over increasing the velocity. With reference to the first Figure-10, which represents the contraction $CR=2$, the stagnation point (point in which the speed of the flow is zero) is found at the beginning of the curvature of the inlet. The streamlines (imaginary lines which correspond to the trajectory of a particle of the flow) show the part of the flow which goes through the nozzle and the part which goes around the structure. The static pressure at this point is at its maximum with respect to the other points of the device. Increasing the contraction to $CR=5$ (second Figure-10) the stagnation point moves even further into the interior of the inlet and the area of high pressure increases. This area of pressure reduces the mass of the fluid which goes through the inlet, in effect, increasing the blocking effect, thereby reducing the actual area of the entrance. In addition, a beginning of separation (separation

bubble) of the flow takes place which leads to greater loss and reduces the efficiency of the device as a whole. This result is present even though the contraction is increased using a smaller throat (tested for $d=0.5m$ on $CR=5.5$ and $CR=7$).

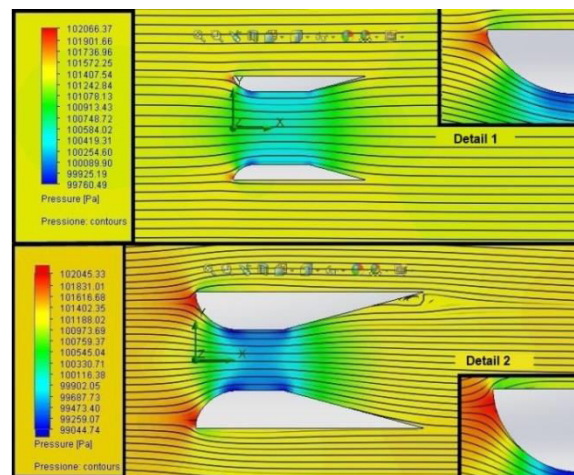


Figure-10. Streamlines and pressure trends for contraction $CR=2$ and $CR=5$ [2].

The maximum velocity reached was 2.15 m/s. In any case attempts were made to improve the convergent-divergent by adding other components. In the end a 2.33 increase in velocity was achieved. This was made possible by adding a second ring diffuser around the Venturi nozzle with a flange fitted around its periphery. An additional conical divergent was added inside the first. Both components are effective when placed at a precise point



with respect to the inlet. As has been repeated on numerous occasions, the power produced by the flow is proportional to the cube root of the flow itself. Therefore, it is reasonable to assume that a mechanism which uses the dynamic nature of a fluid in movement around a structure will be able to increase that fluid's velocity. In other words, if we are able to capture and concentrate the energy of water locally, the exit power of the water when leaving the turbine can be increased significantly. The question that then came to mind was whether or not it would be possible to improve the device by an opportune varying of the geometry of the ISO 5167-3. In the literature there seemed to exist a promising solution. Ohya Y. *et al* (2010) [7] suggest a flange (called wind-lens) placed on the periphery of a diffuser (Figure-11).



Figure-11. DAWT turbine with wind-lens [7].

To improve the average velocity, it was decided to modify the structure of the device by inserting a flange at the exit of the divergent. The reason for adding this attachment is to permit an accelerated flow upon exiting the divergent without being hampered by the slower flow encountered on the outside. In fact, a region of low pressure formed by a strong vortex behind the flange attracts a greater mass of fluid toward the throat inside the device. The simulations carried out with *SolidWorks* confirm the efficacy of the system combined with the ISO 5167-3 geometry. Ohya Y. *et al.* (2010) [7] use straight flanges with $h \geq d * 0.1$. In any event, in our case we designed an flange tempered by a fitting with a radius equal to its width/ height (symbol *S*). This proved to be more effective (+ 0.8%). In addition, since the flange is the part of the structure that is most stressed it results in improved advantages of resistance. Table-4 below shows the velocities reached with the help of this type of flange varying the *h*. As is shown, up to $h=0.480$ m there is an increase of 6.9% in the average velocity. Afterwards, there are no evident or significant advantages to increasing the height. Figures 12(a) and (b) show the depression effect that the flange, expressly designed for our nozzle, produces at the divergent outlet with respect to the initial geometry ISO 5167. What is more, the parameter S_A goes from a value of 0.81 to 0.85 which means that the mass of fluid becomes increasingly drawn towards the inside of the device.

Table-4. Results from an ISO 5167-3 nozzle with flange S (curved) and D (straight) [2].

	$V_m^{(17)}$	V_m^{Inlet}	$C_A^{(18)}$	$S_A^{(20)}$	$B^{(19)}$	$P_A^{(22)}$
h=0.00 S	2.1476	0.9693	1.79	0.81	1.31	2.44
h=0.24 S	2.2488	1.0043	1.87	0.84	1.25	2.80
h=0.36 S	2.2963	1.0189	1.91	0.85	1.23	2.98
h=0.36D	2.2777	1.0106	1.90	0.84	1.24	2.91
h=0.48 S	2.3080	1.0226	1.92	0.85	1.22	3.03

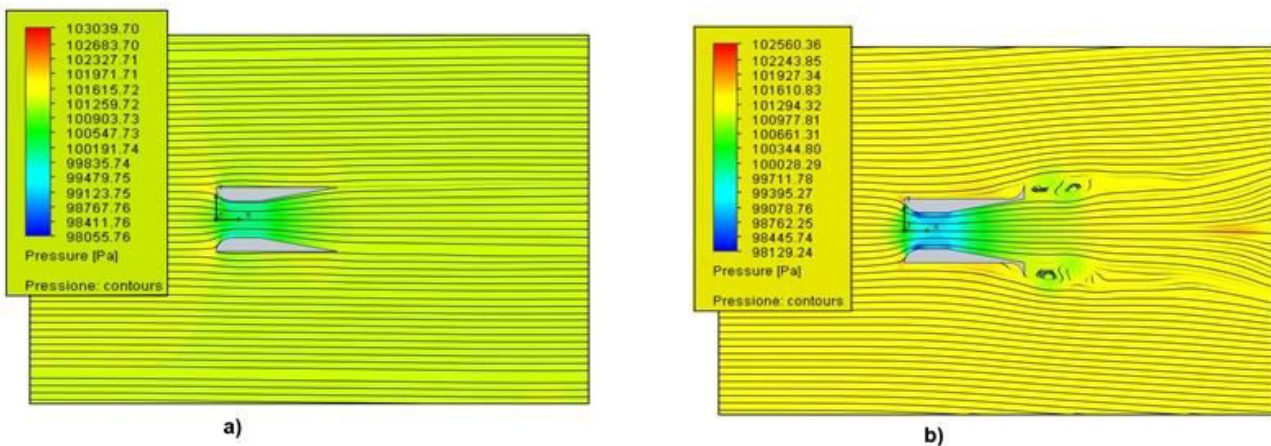


Figure-12. Flow behavior exiting the divergent without flange (a) and with flange S (b) [2].



Since the major inconvenience of the device stems from the blocking effect (given the presence of the convergent) it was decided to add a specifically designed diffuser around the first nozzle at a certain distance from the entrance (Figure-14). The idea is to attract a bigger flow near the throat, accelerating it, creating a depression similar to an air extractor. Looking at Figure-13, we can see the extended area of low pressure that extends from

the final section of the divergent which is equal to the length of the device itself. We can also observe the two ample von Karman vortices that are formed. The correct positioning of this second diffuser becomes critical since we need to find the correct compromise between a greater blocking effect and amplification of velocity obtained (see Table-5).

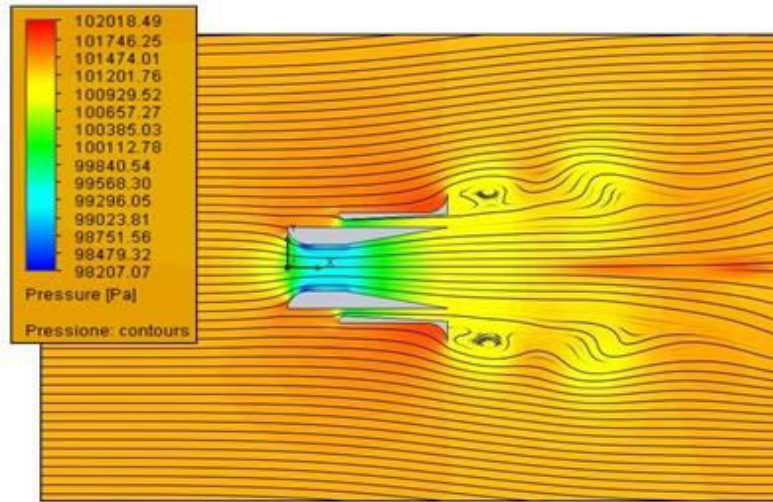


Figure-13. Effect of the secondary diffuser with a flange on the exiting flow of the divergent [2].

The optimal position of the secondary diffuser is found to be that in which the plane of its throat is aligned on the same plane as the exit section of the throat of the main nozzle. On its own, the second diffuser, whose chosen angle is $\varphi_2 = 6^\circ$ (or a value between $4-8^\circ$) seems to yield either no or only very few advantages. When paired with flange S, however, there is an average increase in effectiveness of 8.7% in addition to increasing efficiency

beyond $h=0.600$ m. The use of this additional system (named R) contributes therefore to a total increase in the average velocity of 21.4% at its maximum value with respect to the simple geometry ISO 5167-3 from which we started. The amplification of power passes from a value of 2.44 to 4.36. The results are shown in Table-5. It is worth noticing the substantial increase of the value S_A which reaches 0.95.

Table-5. Results of the nozzle with a secondary diffuser and flange (R20-S) [2].

Ver. [R]	$V_m^{(17)}$	V_m^{Inlet}	$C_A^{(18)}$	$S_A^{(20)}$	$B^{(19)}$	$P_A^{(22)}$
$h=0.36$ S	2.4873	1.0913	2.07	0.91	1.13	3.79
$h=0.48$ S	2.5189	1.1070	2.10	0.92	1.12	3.93
$h=0.60$ S	2.6011	1.1354	2.17	0.95	1.08	4.33
$h=0.72$ S	2.6062	1.1354	2.17	0.95	1.08	4.36

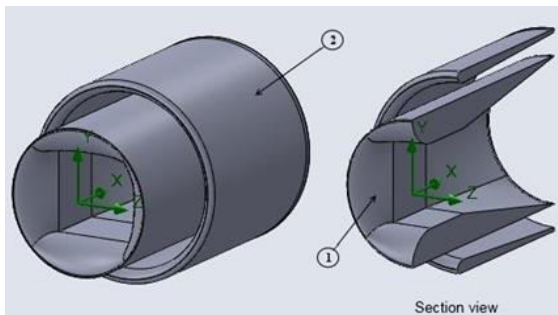


Figure-14. Main nozzle (1) with secondary diffuser(2) [2].

According to ISO 5167-3, the maximum angle of the divergent should be equal to or less than 30° . Reducing it, as shown above (Table-4), the average velocity tends to increase to the detriment of the length of the divergent and therefore, to the device as a whole. In fact, the divergent results in being the longest section of the device. David L. *et al.* (2006) [3] through simulations using various diffusers for wind generators have identified the best ratio between the area of the throat section and the area of the exit area of the diffuser is shown to have a value of 1.56 with an optimum angle of exactly 20° . Using this ratio substantially shortens the diffuser. In any event, applying



this solution to the version with geometry ISO 5167-3 leads to a pronounced worsening of the parameters (-23.8% in average velocity and -89% in power amplification).

The configuration with a second diffuser was shown to be very effective; leading us to the idea of adding an additional (circular) divergent inside the first (called DDi) in order to accelerate the flow exiting from the throat section, precisely at the moment in which it has yielded kinetic energy to the turbine blades. This results in creating another pressure drop in the first section of the main divergent in a way that would "suck" more flow into the throat. In any event the flow is eased in leaving the area, thanks to the low pressure generated by the second flanged diffuser, allowing it encounter a lower gradient of adverse pressure at the outlet. This solution, tested on the version of 20°, was shown to increase the average velocity even further. The best results were obtained when the φ_3 of this internal conical diffuser was as follows:

$$\varphi_3 = \frac{\varphi_1}{2} \quad (23)$$

Where φ_1 is the angle of the main divergent. Another necessary criterion is the precise positioning of the inlet. Three positions were tested:

- On a vertical plane, coinciding to the outlet plane of the throat - this gave lower results as would be expected since this position limits the use for which the DDi was devised as well as not being suitable for the positioning of a Darrieus;
- In the center of the main divergent - this yielded

- results similar to the above. Most likely the position is too far back to obtain maximum benefit;
- At midpoint along the total length of the nozzle – this was demonstrated to be the most effective.

Figure-15 shows the section of the final device with an internal diffuser (with longest maximum length) in position 3, while table 6 reports the results and the related parameters of comparison. As can be seen, this solution increases the V_m to 2.70 m/s; in addition, the parameter S_A reaches a maximum value of 0.99 corresponding to an entrance velocity of around 1.19 m/s which is near the flow asymptotic speed. The blocking effect is reduced to a minimum. This configuration results in an increase in velocity equal to 2.25 and an amplification of power equal to 4.86.

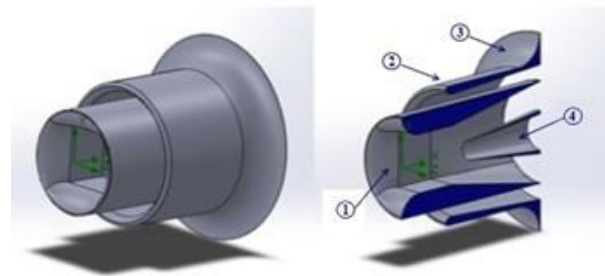


Figure-15. Section view of the final configuration. (1) Main Venturinozzle - (2) Secondary diffuser R - (3) Flange S - (4) Internal diffuser DDi.

Table-6. Results of the version with a conical internal divergent (DDi)^[2].

[R DDi]	$V_m^{(17)}$	V_m^{Inlet}	$C_A^{(18)}$	$S_A^{(20)}$	$B^{(19)}$	$P_A^{(22)}$
$h=0.00 \varphi_3=10^\circ$	2.2588	1.0109	1.88	0.84	1.25	2.84
$h=0.48 \varphi_3=10^\circ$	2.6494	1.1693	2.21	0.97	1.06	4.58
$h=0.60 \varphi_3=8^\circ$	2.6530	1.1684	2.21	0.97	1.06	4.60
$h=0.60 \varphi_3=10^\circ$	2.6897	1.1829	2.24	0.99	1.05	4.79
$h=0.72 \varphi_3=10^\circ$	2.7032	1.1883	2.25	0.99	1.04	4.86

Finally, given that a circular throat has been shown to be more efficient than a square one, it was decided to run the simulation with this type of throat section in order to possible substitute a Darrieus turbine with a Kaplan type bulb propeller. This version, with a $h=0.600$ m flange obtained an increase in average velocity of 2.33 ($V_m=2.79$ m/s) and a power amplification of 5.36. In addition it is 0.2 m narrower and approximately 0.8 m shorter than the square configuration. This corresponds to a possible 12.7 fold increase in power yield compared to a turbine without channelization. Figure-16 shows a rendering of the final configuration.

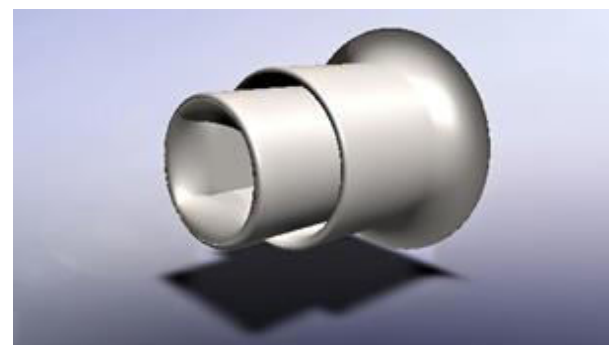


Figure-16. Rendering of the final configuration (R20-S600-DDi10)^[2].



Estimate and costs of potential energy production

In Table-7 are reported an indication of the costs of our device to which must be added the costs of installation and assembly. Choosing the most expensive solution, with a specific alternator allowing for the coupling of the turbine directly to the generator without the aid of a gearbox, the price would be around € 2,700.00. A possible selling price would be around € 5,400.00 for a total initial investment of € 5,900.00 per unit, assuming an expenditure of € 500.00 for each installation. The device has a nominal power output of 4.4kW with a constant and continuous flow. Given the cost of energy to the consumer is on average 0.14 €/kWh, the annual return on investment would be € 5,396.00. The payback period corresponding to the time needed to recover the initial investment (in years) would be:

$$PBP = \frac{\text{Initial investment}}{\text{Average annual return}} \approx 1.1 \quad (24)$$

In addition, since this is renewable energy of a power less than 1 MW, it qualifies for government subsidies for 20 years on the excess kW produced. What's more, since the nominal power is between 1 and 20 kW, this incentive corresponds to the favorable GSE rate of € 0.257/kWh [5]. Taking into consideration an average use of 3 kW (equal to the consumption of a normal city household) it is possible to supply the grid with a surplus of 1.4 kW yielding additional earnings of € 3,152.00, after taking into account the initial expense for the certified grid tie connected inverter, reducing the PBP even further.

Table-7. Component cost table [2].

Ball-bearings (x2)	≈ € 140.00
Screws M4 (x12)	≈ € 5.00
Screws M6 (x14)	≈ € 6.80
Materials in AISI 316 L (2.21 €/kg)	≈ € 513.00
1) GingLong PMG 5000 (5kW) Alternator	≈ € 2,078.00
2) Faurndau PMG 100 S Generator	≈ € 300.00
Gearbox (8:1)	≈ € 300.00
	1) €2,742.80
	2) €1,264.80

The cost per kW of the hydro power plant can be calculated and compared with other renewable energy plants:

$$\frac{\text{Final power plant cost}}{\text{kWh produced}} = 1,340.00 \text{ €/kWh} \quad (25)$$

Average market prices (for power <5kW) for wind power generator ranges between 3,000 - 4,000 €/kW, while those for a photovoltaic panel range between 1,500 - 2,000 €/kW. It thus appears that our system is also

advantageous from the point of view of the cost per power produced. In addition, unlike other sources of energy production it is continuous throughout the day.

CONCLUSIONS

The project was carried out "virtually" using CFD software and programs written *ad hoc* in *Matlab* language. The innovative convergent-divergent based on a Venturi nozzle described by the DIN EN ISO 5167-3:2003 standards (necessary for increasing the velocity of a river which would, otherwise, be too slow to allow any free flow turbine to extract enough power) is capable of increasing the speed of the flow entering a VAWT up to a maximum of 2.25 times with an 11.4 fold increase in power output. A basic three blade turbine with a symmetric profile NACA 0021, to be housed in the throat of the nozzle and with a solidity equal to 0.27 for a diameter of 0.9 and a height of 1.2 m with a C_p of 0.41 at TSR 3.6 supplies a nominal power output of 4.4 kW when the average speed of the water source is 1.2 m/s compared to only 0.4 kW produced without the use of the flow accelerator described in this paper. We have effectively tested a nozzle configuration suitable for the substitution of a vertical axis turbine with a horizontal axis turbine. The nozzle, which in this case has a circular throat, has been shown to increase the flow velocity by a factor of 2.33, increasing the power output by an incredible factor of 12.7. Based on our estimates, this system is economical and more advantageous when compared to other renewable energy systems of equal power, such as solar and wind which are also not able to guarantee continuous energy production during the entire 24 hour period of a day.

Symbols

Symbol	Description	Unit
C_p	Turbine power coefficient	[a]
E_k	Kinetic energy	[J]
m	mass	[kg]
V	Mean velocity	[m/s]
P_{Th}	Theoretical power output	[W]
\dot{m}	Mass flow	[kg/s]
ρ	Fluid density	[kg/m ³]
A_1	Inlet area	[m ²]
A_2	Throat area	[m ²]
T	Torque	[N m]
ω	Angular velocity	[rad/s]
V_1	Mean velocity at inlet	[m/s]
V_2	Mean velocity at throat	[m/s]
p	Static pressure	[Pa]
CR	Contraction ratio	[a]



D	Inlet diameter	[m]
d	Throat diameter	[m]
β	Throat/inlet diameter ratio	[a]
φ_1	Main divergent angle	[°]
φ_2	Secondary divergent angle	[°]
φ_3	Internal divergent angle	[°]
V_m	Weighted average velocity	[m/s]
C_A	Velocity augmentation parameter	[a]
B	Blocking effect parameter	[a]
S_A	Suction effect parameter	[a]
P_A	Power augmentation parameter	[a]
h	Flange height	[m]

- [8] Riegler G. 1983. Principles of energy extraction from a free stream by means of wind turbines. *Wind Engineering*. 7(2): 115-126.

REFERENCES

- [1] Beller C. 2007. Layout design for a Venturi to encase a wind turbine, integrated in a high rise. Diploma thesis University of Stuttgart, Germany. Accomplished at Riso National Laboratory Sustainable Energy.
- [2] Clarke R. 2015. Studio di ottimizzazione di una turbina idraulica a flusso libero. Degree thesis in Aerospace Engineering. University of Bologna, scientific center of Forlì, Italy.
- [3] David L. F. Gaden and Eric L. Bibeau. 2006. Increasing Power Density of Kinetic Turbines for Cost effective Distributed Power Generation. Department of Mechanical and Manufacturing Eng., University of Manitoba, Canada R3T 5V6. http://home.cc.umanitoba.ca/~bibeauel/research/papers/2006_Gaden_powergen.pdf.
- [4] DIN EN ISO 5167-3:2003. Measurement of fluid flow by means of pressure differential devices inserted in circular cross-section conduits running full - Part 3: Nozzles and Venturi nozzles.
- [5] Gestore Servizi Energetici. 2012. Rapporto statistico impianti a fonti rinnovabili. Italia. Italy.
- [6] Newman B.G. 1983. Actuator-disc theory for vertical-axis wind turbine. *Journal of Wind Engineering and Industrial Aerodynamics*. 15: 347-355.
- [7] Ohya Y., Karasudani T. and Zhang X. 2010. A Shrouded Wind Turbine Generating High Output Power with Wind-lens Technology. *Energies* 2010, 3, 634-649; doi: 10.3390/en3040634.